2

Architectural Design of Quantum Cellular Automata to Implement Logical Computation

Alejandro León
Facultad de Ingeniería, Universidad Diego Portales Ejército 441, Santiago Chile

1. Introduction

The limits to miniaturization of electronic devices are reached with sizes where quantum mechanics rules over the dynamics of the system. Because of this, enormous efforts are being made in search of new technologies to store and process information that can efficiently replace classic electronics. The proposal for quantum systems for carrying out computation represents an attempt to create a new generation of information processors (Nielsen & Chuang, 2003). The major advantage of quantum computation is that it can resolve numeric problems that cannot be resolved by classical computation. However, there remains the unresolved problem of the coherence of the proposed systems. Some significant advances have been made in addressing these problems using dislocated qubits with global control protocols (Fitzsimons et al., 2007), with small molecular systems.

On the other hand, a completely different solution to quantum computation has been attempted using cellular automata architecture to develop classical computational processes with quantum entities. Important advances have been made with automata based on quantum dot arrays (QCA), the idea for which was proposed by C. Lent and collaborators (Lent et al., 1993). The original idea was introduced as a system of quantum corrals with

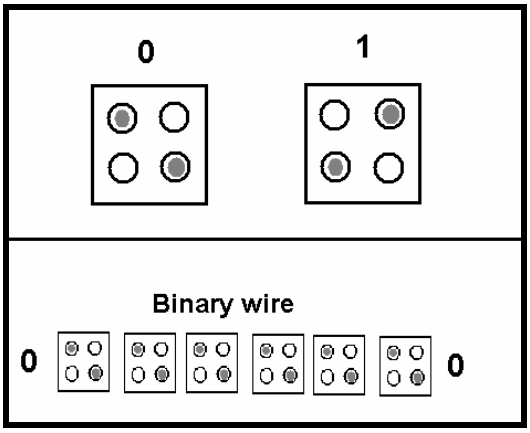

Fig. 1. Quantum dot scheme proposed by the Lent group.

four quantum dots inside it and doped with two electrons. The electrons can tunnel through the quantum dots, but cannot get out of the corrals that form the cells of the automata. This architecture can propagate and process binary information with adequate control protocols (Csurgay et al., 2000). Figure 1 shows a scheme of the original idea of the Notre Dame group.

We can appreciate from Figure 1 that the cell that makes up the cellular automata is composed of four quantum dots and that the two extra electrons in the cell can locate themselves in any of the four quantum dots. Owing to Coulomb interaction between the electrons, the minimum energy configurations of the cell correspond to the diagonals of a square. This allows for defining a 0 logic state and another state that corresponds to 1 logic (the two diagonals). Figure 2 shows the implementation of two important classical logic gates using this architecture.

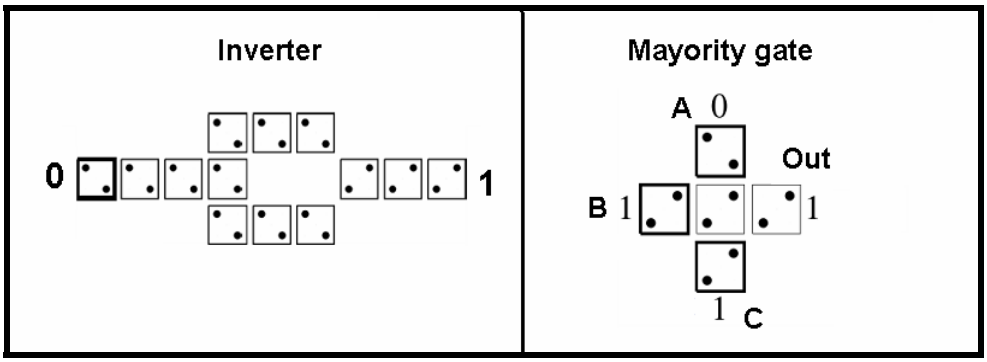

Fig. 2. Scheme of the implementation of the inverter gate and the majority gate with the architecture proposed by the Lent group.

The first experimental demonstration of the implementation of a QCA was published in 1997 (Orlov et al., 1997). A subsequent work also demonstrated an experimental method for the implementation of a logic gate (Amlani et al., 1999), and a shift register was also reported (Kummamuru et al., 2003). These results provide good agreement between theoretical predictions and experimental outcomes at low temperatures. Implementation at room temperature requires working at the molecular level, and in the context of molecular cellular automata; there are also important contributions at the experimental level (Jiao et al., 2003). In the molecular case, the quantum dots correspond to oxide reduction centers, and as in the case of metallic quantum dots or semiconductors are operated with electrical polarization. The implementation of this cellular automata architecture is achieved with complex molecules, supported in a chemically inert substrate. The implementation is achieved in an extremely small chain of molecules (Jiao et al., 2003). Another implementation at room temperature corresponds to an array of magnetic quantum dots that can propagate magnetic excitations to process digital information (Macucci, 2006). These systems use the magnetic dipolar interaction among particles whose size is at the submicrometer scale. A theoretical study was recently published about the behavior of cellular automata composed of an array of polycyclic aromatic molecules (León et al., 2009), using the polarization of electronic spin. In this work it is established that by increasing molecules in one of the directions of the plane, forming graphene nanoribbons, binary

information can be transmitted at room temperature. The disadvantage of the proposed system is that the nanoribbons will reach sizes on the order of micrometers and consequently the miniaturization of the circuits will be only partial.
In this work we propose a cellular automata with graphane structured molecules and graphane nanoribbons to propagate and process digital information. The cells that make up the architecture of the automata correspond to the molecules and to sections of the nanoribbon. We intend to verify theoretically that the proposed system is scalable and binary information can be stored, propagated and processed at room temperature.

2. Graphene and Graphane

2.1 Graphene and Graphene Nanoribbons

Graphene is a simple bidimensional structure of carbon atoms. In 2004 the group of Kostya Novoselov (Nonoselov et al, 2004) succeeded in isolating a simple layer of graphene using a technique by mechanical exfoliation of graphite. This work represented the beginning of many theoretical and experimental studies and their potential applications to systems derived from graphene (Geim, 2009; Castro Neto et al., 2009). A schematic view of the graphene is shown in figure 3.
Recent studies have shown than the electronic structure of graphene nanoribbons (GNRs) exhibits remarkable geometric-dependent properties: it can have metallic or semiconductor behavior depending on the ribbon width and on the arrangement of the atoms on its side edges. It has been demonstrated that the transport and optical properties of GNRs are strongly affected by the edge shape, in particular in the case of ribbons with zigzag edges due to the existence of localized edge states which gives a sharp peak in the density of states at the Fermi level (Nakada et al., 1996; Wakabayashi, 2001). Different device junctions based on patterned GNRs have been proposed (Wang et al., 2007; Ren et al., 2007; Silvestrov & Efetov, 2007) and constructed which can confines electronic states realizing quantum-dot like structures. The electronic states of these confined GNRs structures can be manipulated by chemical edge modifications or impurities addition. A schematic view of the GNRs is shown in figure 4.

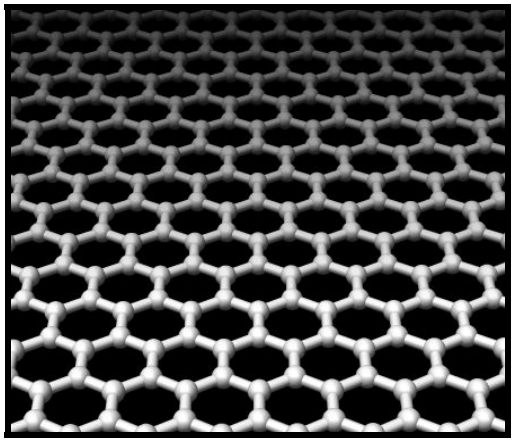

Fig. 3. Scheme of the graphene.

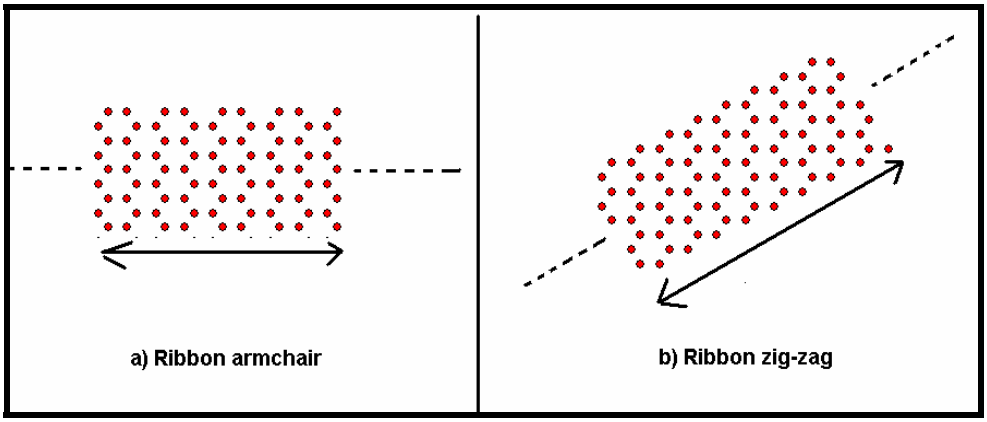

Fig. 4. Scheme of the graphene nanoribbons with armchair and zig-zag edges.

2.2 Graphane

A theoretical investigation in 2007 (Sofo et al.,2007) predicted a new form of graphene totally saturated with hydrogen. The authors of this paper give the name "graphane" to this new form derived from the graphene. The shape of this new structure is similar to graphene, with the carbon atoms in a hexagonal lattice and alternately hydrogenated on each side of the lattice. Figure 5 shows a scheme of this structure.

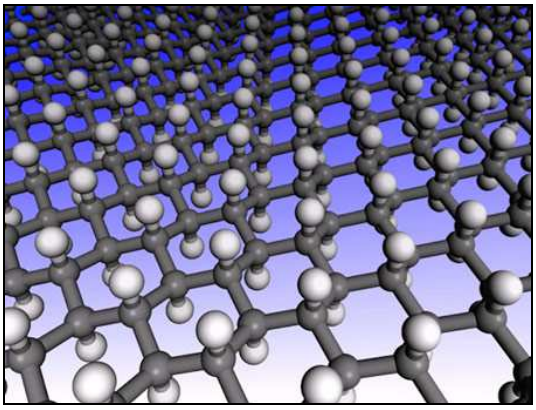

Fig. 5. Scheme of graphane. The gray spheres represent carbon atoms and the white spheres represent hydrogen atoms.

In January 2009, the same group that isolated graphene in 2004 published a paper in Science magazine reporting the hydrogenation of graphene and the possible synthesis of graphane (Elias et al., 2009). Since then there has been growing scientific interest in the study of hybrid graphene-graphane systems and their potential applications (Singh & Yakobson, 2009; Li et al., 2009; Lu & Feng, 2009; Balog, 2010). In this chapter we will discuss graphene nanoribbons and hydrogenated graphene nanoribbons according to the graphane structure. We can imagine these structures as a ribbon-like bidimensional graphane structure. The

atoms of the edges of the ribbon are connected to hydrogen atoms to passivate the free bond. The other system studied in this research is polycyclic aromatic molecules (León, 2009), and polycyclic aromatic molecules but with hydrogen atoms alternately bonded to carbon atoms such that they can be considered as a section of rectangular graphane.

3. Graphene Nanoribbon array in a cellular automata architecture with spin polarization

In this work we propose the implementation of a cellular automaton with cells containing graphene nanoribbons (GNRCA). This kind of carbon-based nanostructures can be obtained by different experimental techniques (Berger et al., 2006; Han et al., 2007; Heersche et al., 2007). In our study we will consider our GNRCA with cells composing by finite GNRs passivated with hydrogen atoms, these structures are also known as polycyclic aromatic hydrocarbons. In Fig. 6 we have displayed two $C_{44}H_{18}$ finite GNRs. The electronic and magnetic properties of the systems are obtained by means of first principles calculations based on the pseudo-potentials method and by using the generalized gradient approximation Perdew–Burke–Ernzerhof with spin polarization (Perdew et al., 1996). All structures are relaxed using the Direct Inversion Iterative Subspace method (Csaszar & Pulay, 1984) with a residual force criteria less than 10^{-4} (Hartree / bohr). Calculations were performed using the OPENMX Code (Openmx, 2007). We found that the minimum energy state of this GNR presents spin polarization along the zigzag-type edges, corresponding to the edges containing more carbon atoms (Son et al., 2006; Jiang et al., 2007; Wang et al., 2008; Fernandez-Rossier & Palacios, 2007). This state is degenerate as it is shown in Fig. 7, therefore we can define the 0 or 1 logical states for the automata.

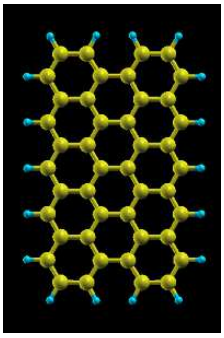

Fig. 6. Molecule $C_{44}H_{18}$

By considering a cluster formed by two interacting finite ribbons we found the distance for which the total energy of the cluster is minimum (figure 8). This energy minimum occurs when the nearer edges of the ribbons have opposite total density spin polarization, i.e., energy states with configurations 00 or 11, we call it the "antiferromagnetic state" (AS). Furthermore, this system also presents a metastable state with spin polarizations of 01 or 10 for neighbor edges with the same type of spin polarization, we call it "ferromagnetic state" (FS). These are the two kinds of states represented in Fig. 7. For this cluster the energy separation between the states FS and AS is ΔE(FS−AS) = 0.0629 meV. This difference in energy is very little as compared with the energy separation between the FS (or AS) state

and the paramagnetic state calculated without spin polarization (corresponding to 278 meV for the molecule of C44H18). This energy difference is shown in Figure 9.

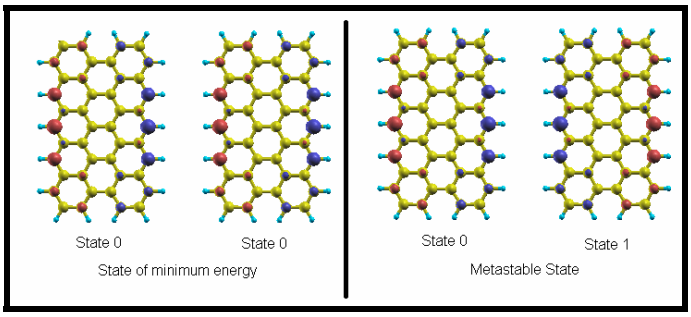

Fig. 7. Minimum energy state (left panel) and metastable state (right panel) for a system of two $C_{44}H_{18}$ molecules. Red balls represent the spin up total density and blue balls represent the spin down total density.

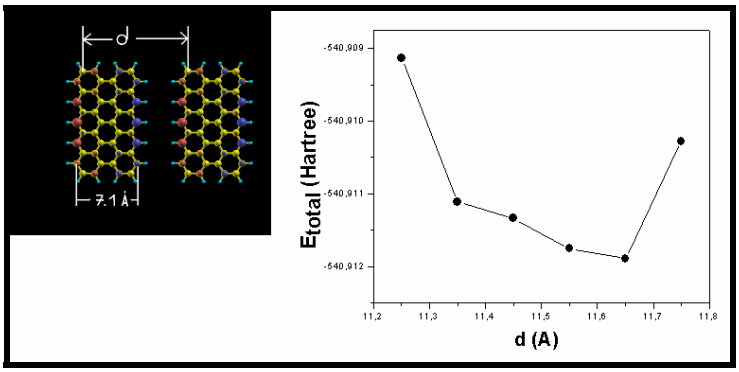

Fig. 8. Study to get the distance that minimizes the energy of the cluster.

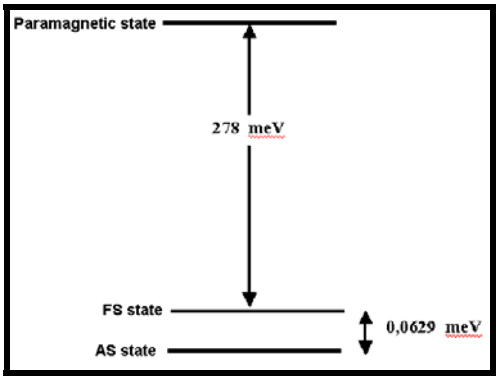

Fig. 9. Energy separation between FS state and the paramagnetic state.

The energy separation between the states AS and FS is usually referred in the cellular automata literature as "kink energy" E_K. In the context of magnetic properties we call it the parameter of "superexchange" between cells $J = E_K$. To postulate these systems as room-temperature binary information processors we have to study the feasibility of this superexchange effect, which we have found for small structures as not limited in scaling. We have performed the same study for longer nanoribbons with more atoms along its zigzag edges. Our results are displayed in Fig. 10 and they indicate that effectively this effect can be scaled to greater size systems. To verify that the scaling works linearly for very long ribbons we have performed first principles calculations for two infinitely long GNRs. To do this we built a tridimensional (3D) crystal but considering only interaction between the two GNRs. Figure 11 shows a scheme in the *X*-*Y* plane, in the *Z* direction the ribbon separation was 15 Å. We consider three unitary cells with a different number of atoms along the zigzag edges N_Z = 9,10,11. Our results show that independent of the size of the unitary cell the normalized *J* parameter is *J*(meV) $/N_Z$ = 0.022 which corresponds to the slope obtained in the case of the finite nanoribbons in Fig. 10.

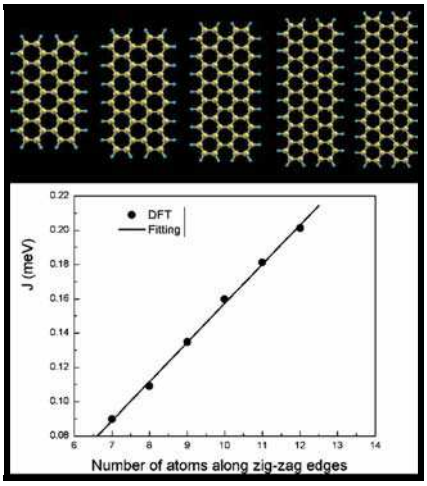

Fig. 10. Superexchange energy parameter of in meV as a function of the number of carbon atoms along the zigzag edges.

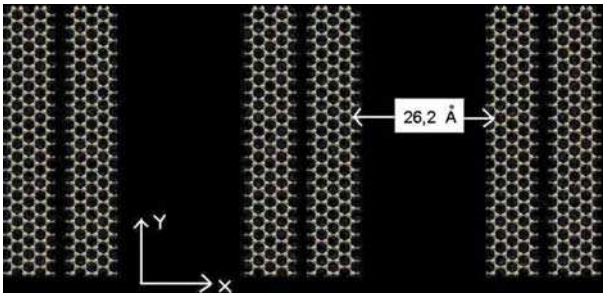

Fig. 11. Scheme in the X-Y plane of the 3D crystal used to perform the calculation of the *J* value for two infinite ribbons in the Z direction the ribbon separation was 15 Å.

The dynamic response of the GNRCA is studied by implementing an "accelerated algorithm for discrete systems" (Krauth, 2006) based in the Glauber dynamics (Glauber, 1963). To perform this study we must define a unit of time for doing the simulation. Due to the phenomenon of spin polarization has a completely quantum origin, we will use the evolution propagator to estimate the time for the signal transmission. The system consisting of two finite GNRs, such as the one shown in Fig. 7, can be seen as a two-level system so a general state of the system can be written as $|\Psi\rangle = a e^{-i\omega t}|0\rangle + b e^{i\omega t}|1\rangle$ with $\omega = \Delta E / \hbar$ where $\Delta E = J$. With this frequency and a threshold J value of 150 meV, we define the time unit adopted in modeling the dynamic behavior of the automaton as $T = \hbar / \pi J \approx 10^{-15}\ s$.

We intend to study the form in the binary information is propagated through a molecular wire formed by N cells. To do this we must have one or more control cells that trigger the change in the state of the GNRCA. By defining nc as the number of control cells that change simultaneously its polarization spin state under an external excitation, then the input parameters for the GNRCA dynamic simulation will be N, nc, J, and the system temperature T. The results indicate the existence of a threshold value for the superexchange parameter J for a given temperature, above that value the automaton state can be changed and it will remain in that state, meanwhile the control cell cannot be changed. The threshold value of J is obtained by the following procedure: (1) for an automaton of N cells (GNRs) and with nc control cells, it is defined as an initial configuration with all cells having the same polarization state (+1 or -1). The magnetization will be given by: $M = (1/N)\sum_{j=1}^{N} m_j$, where m_j is the polarization of each cell. (2) For a temperature T and a given value of J, the control cell polarization is reversed and an average value for the magnetization of the whole automaton is calculated for a sufficiently long time (infinite time compared with the automaton operation time). The top panel of Fig. 12 shows the study for automata with 3, 4, 5, and 6 cells, and one control cell ($n_C = 1$). All cells are in an initial configuration -1. The polarization of the first cell is changed to +1 and then it is waited for t =30 ps. We can see that for all values of the parameter J, the average magnetization is always positive because the polarization of the control cell remains fixed in +1, and the rest oscillates between -1 and +1. For the molecular automaton that works as a cable, it is expected that once the polarization of the control cell changes, the other cells also change and they remain in the new state of polarization (meanwhile the polarization of the cell control does not change). In the study illustrated in the Fig. 12 it is observed that for T=300 K the J value for which that state is reached is close to J =150 meV for all automata. This value increases with the number of cells in the automaton, as shown in the bottom panel of Fig. 12 for automata with nc =1 and N = 7, 8, 9, and 10, respectively. To obtain this value for J the former study of scaling shows that it would be required ribbons of an approximated length of 2.1 μm along the zigzag edges.

Figure 13 shows a simulation for an automaton with a variable number of control cells. The figure displays the time (in picosecond) that the signal takes to go from one end to the other as a function of the number N of cells for T =300 K, J=150 meV, and nc from 1 to 4. It can be observed that the time increases exponentially with the number of cells N and it decreases linearly with the number of control cells. In this way we can postulate a molecular cable to transmit digital information. Figure 14 shows a diagram of the molecular wire.

This study shows that it is possible to propagate binary information through cellular automata based on carbon based nanostructures. We have analyzed other types of shaped

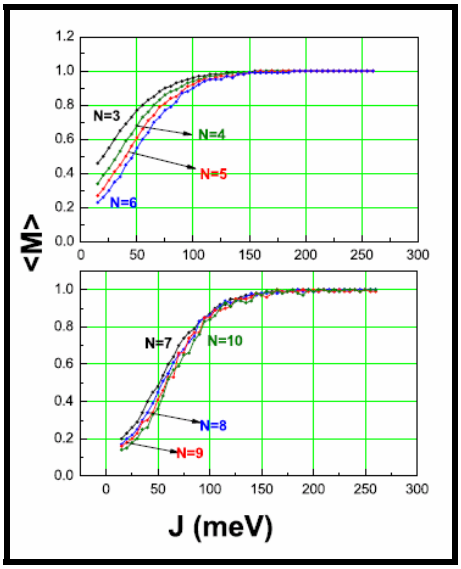

Fig. 12. Upper panel shows the average of the magnetization as a function of J for automata with one control cell and N = 3, 4, 5 and 6 cells, respectively. Lower panel the same study for automata with N = 7, 8, 9 and 10 cells.

graphene fragments, for instance triangular structures (figure 15) that have the advantages of having an even number of them in the automaton, an inverter logic gate could be automatically implemented. Other structures studied are Z-shaped (figure 16) ribbons (León et al., 2008) and antidot lattices formed by holes with zigzag edges on a graphene nanoribbon (Rosales et al., 2009). The disadvantage of these types of clusters arises from the difficulty in the synthesis process and scaling. The systems of graphene nanoribbons

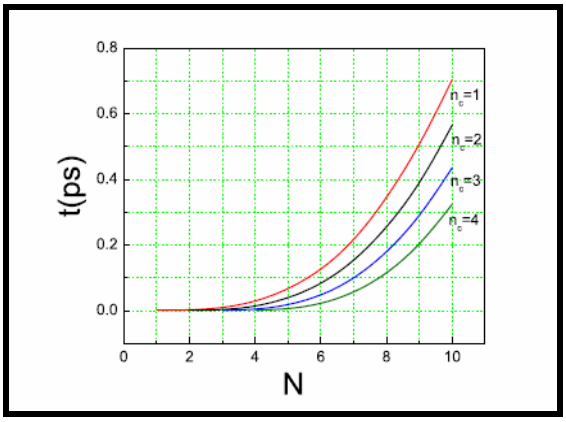

Fig. 13. Time taken by the signal to travel from one end to the other of the automaton as a function of the total number of cells The simulation was performed for J = 150 meV and T = 300 K. Different curves represent simulations with distinct number of control cells.

proposed in this work are scalable for working at room temperature. Besides, standard lithographic techniques and other controlled cutting processes (Ci et al., 2008) can be used for creating graphene nanoribbons with zigzag edges and length desired.

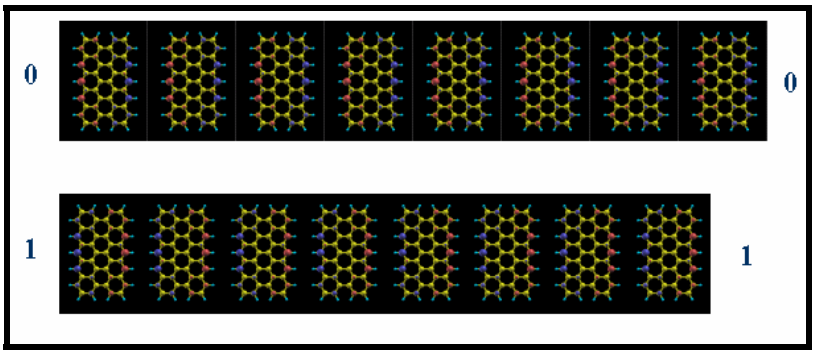

Fig. 14. Molecular wire.

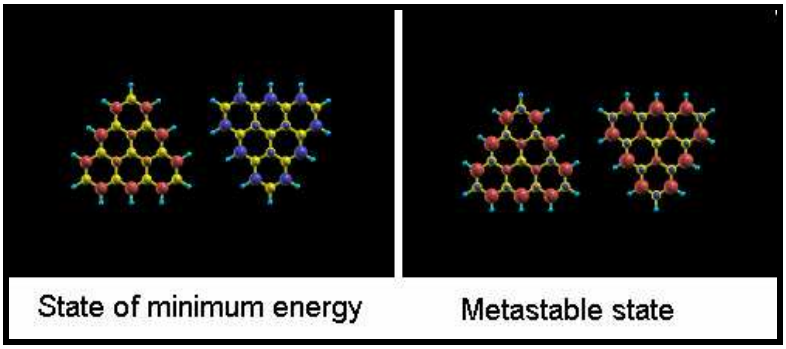

Fig. 15. Triangular structures.

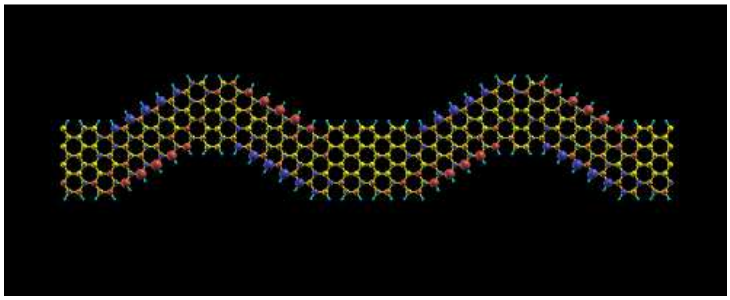

Fig. 16. Structures Z-shaped ribbons.

4. Graphane Nanoribbon array in a cellular automata architecture with electric polarization

4.1 Quantum dots in graphane nanostructures

The role of quantum dots in the studied nanostructures will be played by oxide reduction centers. These centers will be obtained by leaving two regions, on opposite edges, with three unhydrogenated carbon atoms. As a result of this, the free electrons will locate themselves in one of the quantum dots if they are confined with an external electrical field. To verify the feasibility of our research we made calculations of the stability of these nanosytems. The results show that these structures are stable at room temperature. Figure 17 shows the scheme of a $C_{28}H_{36}$ molecule with two quantum dots of the type previously described. In this figure, we can appreciate the isosurface of the HOMO for a determined value, when the molecule is in an electrical field of 1.0 GV/m according to the direction in the figure.

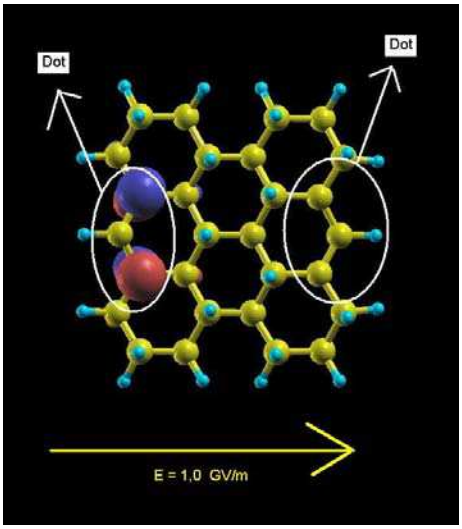

Fig. 17. Scheme of a hydrogenated aromatic molecule, except in the regions where quantum dots are located.

In the case of the graphane nanoribbon, the regions with two quantum dots will be separated by a region sufficient to create an infinite barrier for the electrons compared to the barrier between the quantum dots (figure 18). This distance should allow for the electrostatic interaction among neighboring cells. The value of this parameter in function of the width of the ribbon, the temperature and the type of substrate that supports the structure are determined in this investigation. In the case of molecular arrays, this distance represents the separation among the mass centers of the molecules. Figure 19 shows a scheme of the quantum dots in the nanoribbons and in the molecular array. The manner of arranging the quantum dots in the ribbon and molecular array allows for propagating information, that is, this structures represent molecular wires to join the different devices that process and store information. The quantum dot arrays in both structures are designed in this investigation to develop universal logic operations and the form of the arrays are designed so that they function as data storing devices.

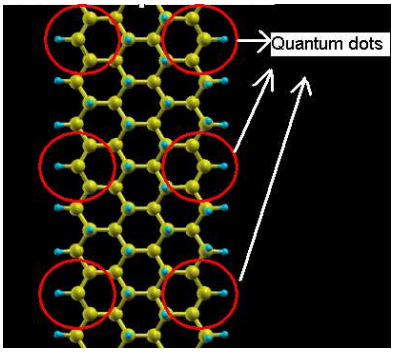

Fig. 18. Scheme of quantum dots in the graphane nanoribbons.

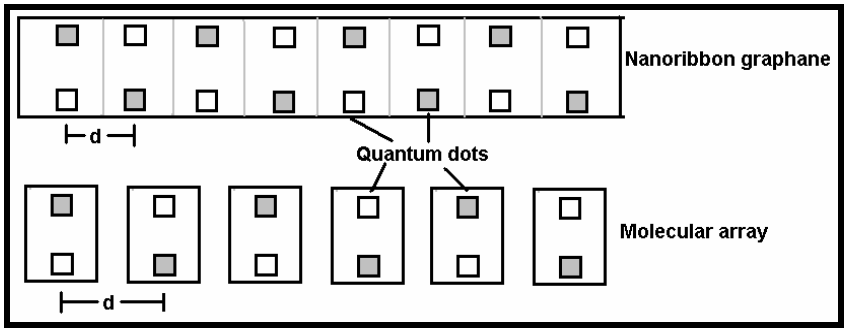

Fig. 19. Scheme of quantum dots in the studied structures

4.2 Electronic and magnetic properties of the Nanoribbons Graphene

The electronic and magnetic properties of the systems are obtained by means of first principles calculations based on the pseudo-potentials method and by using the generalized gradient approximation Perdew–Burke–Ernzerhof with spin polarization (Perdew et al., 1996). All structures are relaxed using the Direct Inversion Iterative Subspace method (Csaszar & Pulay, 1984) with a residual force criteria less than 10^{-4} (Hartree / bohr). Calculations were performed using the OPENMX Code (Openmx, 2007). Figure 20 shows the result of the calculation for a neutral nanoribbon. The zero energy corresponds to the Fermi level. We can see that the electrons with energy near the Fermi level, are located on both sides of the nanoribbon. Analyzing Figure 21, we see that the ground state of the system is degenerated to the value of spin. This means that if we remove an electron from the unit cell, we have a system with two quantum dots and an electron tunneling between quantum dots.

The calculations of the electronic properties of a cell (molecule) show that in the presence of an electric field (polarization of the neighboring cell), electric charge is located, as shown in Figure 22.

The calculation of the interaction energy between two consecutive cells for the nanoribbons and the molecular arrangement is about 540 meV. This implies that we can spread information through the cellular automata at room temperature.

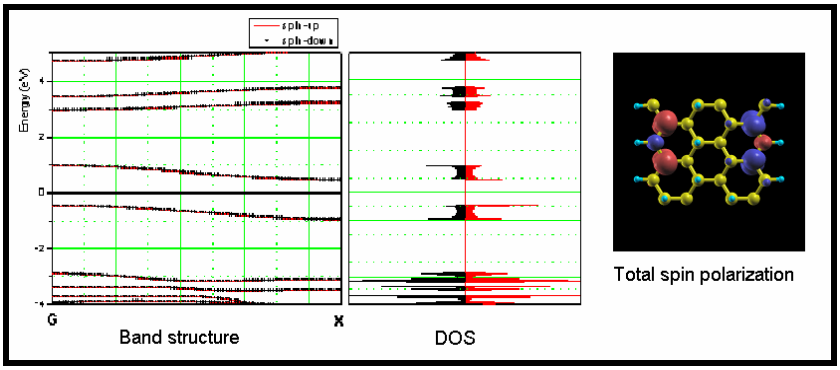

Fig. 20. Band structure, density of states and total spin polarization of the unitary cell.

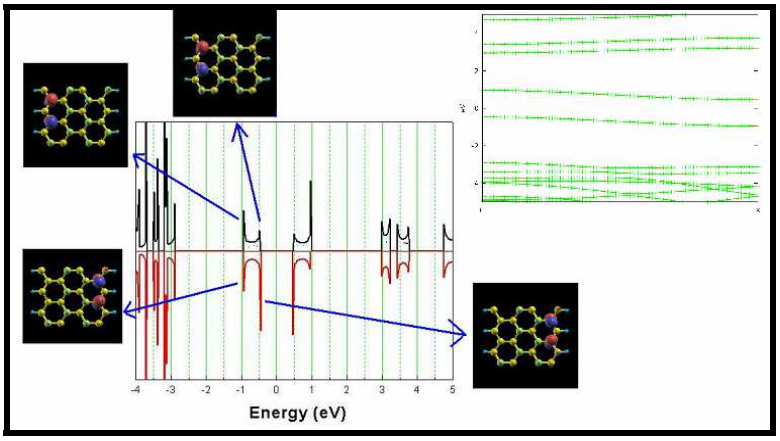

Fig. 21. Real part of the wave function, density of states and band structure for neutral nanoribbon.

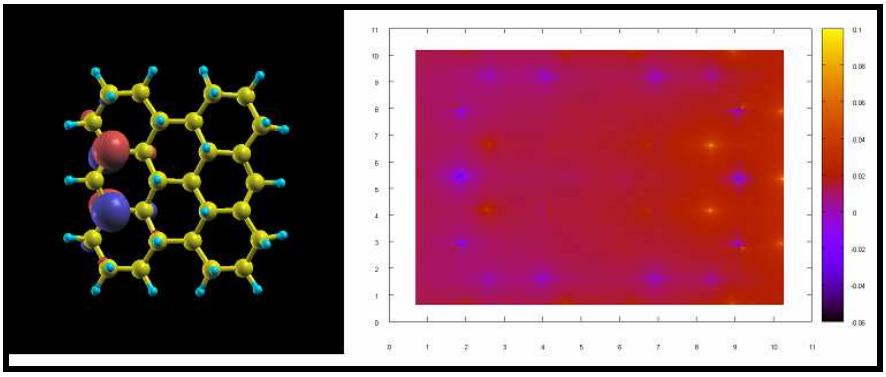

Fig. 22. HOMO and excess of electrical charge in the molecule E = 1,0 GV/m Q = + 1

5. References

Amlani, I.; Orlov, A. O.; Toth, G.; Bernstein, G. H.; Lent, C. S. & Snider, G. L. (1999). *Science* 284, 289.

Balog, R.; Jørgensen, B.; Nilsson, L.; Andersen, M.; Rienks, E.; Bianchi, M.; Fanetti, M.; Lægsgaard, E.; Baraldi, A.; Lizzit, S.; Sljivancanin, Z.; Besenbacher, F.; Hammer, B.; Pedersen, T. G.; Hofmann, P. & Hornekær, L. (2010). *Nature Materials* 9, 315.

Berger, C.; Song, Z.; Li, X.; Wu, X.; Brown, N.; Naud, C.; Mayou, D.; Li, T.; Hass, J.; Marchenkov, A. N.; Conrad, E. H.; First, P. N. & de Heer, W. A. (2006). *Science* 312, 1191.

Castro Neto, A. H.; Guinea, F.; Peres, N. M. R.; Novoselov, K. S. & Geim, A. K. (2009). *Rev. Mod. Phys.* 81, 109.

Ci, L.; Xu, Z; Wang, L.; Gao, W.; Ding, F.; Kelly, K. F.; Yakobson, B. I. & Ajayan, P. M. (2008). *Nano Res.* 1, 116.

Csurgay, A. I.; Porod, W. & Lent, C. S. (2000). *IEEE Trans. On Circuits and Systems* I 47, 1212.

Elias, D. C.; Nair, R. R.; Mohiuddin, T. M. G.; Morozov, S. V.; Blake, P.; Halsall, M. P.; Ferrari, A. C.; Boukhvalov, D. W.; Katsnelson, M. I.; Geim, A. K. & Novoselov K. S. (2009). *Science* 323, 610.

Fitzsimons, Xiao, L.; Benjamin, S. C. & Jones J. A. (2007) *Phys. Rev. Lett.* 99, 030501.

Geim, A. K. (2009). *Sience* 324, 1530.

Glauber, R. J. (1963). *J. Math. Phys.* (Cambridge, Mass.) 4, 294.

Han, M. Y.; Özyilmaz, B.; Zhang, Y. & Kim, P. (2007). *Phys. Rev. Lett.* 98, 206805.

Heersche, H. B.; Jarillo-Herrero, P.; Oostinga, J. B.; Vandersypen, L. M. K. & Morpurgo, A. F. (2007), *Nature* 446, 56.

Jiao, J.; Long, G. J.; Grandjean, F.; Beatty, A. M. & Fehlner, T. P. (2003). *J. Am. Chem. Soc.* 125, 7522.

Krauth, W. (2006). *Statistical Mechanics: Algorithms and Computations* (Oxford University Press, New York).

Kummamuru, R. K.; Orlov, A. O.; Ramasubramaniam, R.; Lent, C. S.; Bernstein, G. H. & Snider, G. L. (2003). *IEEE Trans. On Electron Devices* 50, 1906).

Lent, C. S.; Tougaw, P. D.; Porod, W. & Bernstein, G. H. (1993). *Nanotechnology* 4, 49.

León, A.; Barticevic, Z. & Pacheco, M. (2009). *Appl. Phys. Lett.* 94, 173111.

León, A.; Barticevic, Z. & Pacheco, M. (2008). *Microelectron. J.* 39, 1239.

Li, Y.; Zhou, Z.; Shen, P. & Chen, Z. (2009). *J. Phys. Chem C* 113, 15043.

Lu, Y. H. & Feng, Y. P. (2009). *J. Phys. Chem C* 113, 20841.

Macucci, M. (2006). *Quantum Cellular Automata*, Imperial College Press, ISBN 1-86094-632-1, London, United Kingdom.

Nielsen, M. A. & Chuang, I. L. (2003). *Quantum Computation and Quantum Information,* Cambridge University Press, ISBN 0-521-63503-9, Cambridge, United Kingdom.

Nakada, K.; Fujita, M.; Dresselhaus, G. & Dresselhaus M. S. (1996). *Phys. Rev. B* 54, 17954.

Nonoselov, K. S.; Geim, A. K.; Morozov, S. V.; Jiang, D.; Zhang, Y.; Dubonos, S. V.; Grigorieva, I. V. & Firsov, A. A. (2004) *Science* 306, 666.

OPENMX (2007). http://www.openmx-square.org.

Orlov, A. O.; Amlani, I.; Bernstein, G. H.; Lent, C. S. & Snider, G. L. (1997). *Science* 277, 928.

Rosales, L.; Pacheco, M.; León, A.; Barticevic, Z.; Latgé, A. & Orellana, P. (2009). *Phys. Rev. B* 80, 073402.

Singh, A. K. & Yakobson, B. I. (2009). *Nano Letters* 9, 1540.

Sofo, J. O.; Chaudhari, A. S. & Barber, G. D. (2007). *Phys. Rev. B 75*, 153401.

Wakabayashi K. (2001). *Phys. Rev. B* 64, 125428.

Cellular Automata - Innovative Modelling for Science and Engineering

Edited by Dr. Alejandro Salcido

ISBN 978-953-307-172-5
Hard cover, 426 pages
Publisher InTech
Published online 11, April, 2011
Published in print edition April, 2011

Modelling and simulation are disciplines of major importance for science and engineering. There is no science without models, and simulation has nowadays become a very useful tool, sometimes unavoidable, for development of both science and engineering. The main attractive feature of cellular automata is that, in spite of their conceptual simplicity which allows an easiness of implementation for computer simulation, as a detailed and complete mathematical analysis in principle, they are able to exhibit a wide variety of amazingly complex behaviour. This feature of cellular automata has attracted the researchers' attention from a wide variety of divergent fields of the exact disciplines of science and engineering, but also of the social sciences, and sometimes beyond. The collective complex behaviour of numerous systems, which emerge from the interaction of a multitude of simple individuals, is being conveniently modelled and simulated with cellular automata for very different purposes. In this book, a number of innovative applications of cellular automata models in the fields of Quantum Computing, Materials Science, Cryptography and Coding, and Robotics and Image Processing are presented.

How to reference

In order to correctly reference this scholarly work, feel free to copy and paste the following:

Alejandro León (2011). Architectural Design of Quantum Cellular Automata to Implement Logical Computation, Cellular Automata - Innovative Modelling for Science and Engineering, Dr. Alejandro Salcido (Ed.), ISBN: 978-953-307-172-5, InTech, Available from: http://www.intechopen.com/books/cellular-automata-innovative-modelling-for-science-and-engineering/architectural-design-of-quantum-cellular-automata-to-implement-logical-computation

INTECH
open science | open minds

InTech Europe
University Campus STeP Ri
Slavka Krautzeka 83/A
51000 Rijeka, Croatia
Phone: +385 (51) 770 447
Fax: +385 (51) 686 166
www.intechopen.com

InTech China
Unit 405, Office Block, Hotel Equatorial Shanghai
No.65, Yan An Road (West), Shanghai, 200040, China
中国上海市延安西路65号上海国际贵都大饭店办公楼405单元
Phone: +86-21-62489820
Fax: +86-21-62489821